



Porous Properties and Surface Chemical Properties of the Modified Biomass Materials

Ling Zhang^{1,2}, Xiaoying Zeng², Tiandong Zhang², Weiyao Hu², Rui Gao², Jianyun Yang¹
and Zhaolin Zhan^{*1}

^{*1} Faculty of Materials Science and Engineering, Kunming University of Science and Technology,
No. 68, Wenchang Road, Kunming 650093, China

² R&D Center, China Tobacco Yunnan Industrial Co. Ltd., No. 367, Hongjin Road, Kunming
650231, China

Email: zhang-874005@163.com

ABSTRACT

Porous material was prepared by carbonization and modification treatment of the residues extracted from tobacco stems. The preparation process of the adsorption material was optimized by response surface method. The structure and properties of the product were characterized by scanning electron microscopy, N₂ adsorption-desorption, infrared spectroscopy. The results showed that: the excellent produced conditions for the adsorption materials are as follows: the temperature is 707.40 °C, the ratio is 1:3 and the time is 17.20 min. The surface of material modified by KOH was a typical porous structure which mainly based on a large number of cavities and pores. The material had high specific surface areas and pore volumes. The material surface was a typical porous structure with a moderate pore size and uniform distribution. The pore structure is mainly based on the larger mesoporous structure and a certain microporous structure. The material with the specific surface areas and pore volumes as high as 1513.27 m²/g and 0.67 cm³/g were obtained. The pore size is concentrated between 6 ~ 15 nm, which belongs to mesoporous materials. The modified material possesses more abundant functional groups, such as -OH, -CH and other functional groups, so that the material has a certain pro-organic. The material can effectively adsorb the tar, CO and phenol in the cigarette smoke, which decreased by 20.5%, 19.2%, 49.66%, respectively. The preparation method is simple and easy to operate, and the raw materials are easy to get. The material has a strong industrial application prospect.

Keywords: Tobacco stem, Residue, Porous materials, Microstructure, Surface properties.

1. INTRODUCTION

Porous materials have very important applications in many fields [1]. Activated carbon, zeolite molecular sieve and active alumina are common porous materials [2, 3]. In addition, some materials are developed for the selective adsorption of certain components [4]. Porous materials are divided into three kinds according to the size of their pore size: the pore size less than 2 nm are microporous materials, the pore size of nm 2~50 are mesoporous materials, and the pore diameter greater than 50 nm are large porous materials [5].

Compared with other porous materials, activated carbon has more developed pore structure and abundant surface active groups. It has larger adsorption capacity and faster adsorption rate, so it has been widely studied and applied. There are many reports on the preparation of activated carbon materials from biomass. With coconut shell as raw material, the activated carbon with a certain proportion of micro- and mesoporosity was prepared by using sodium hydroxide aqueous solution [6].

With gelatin and starch as raw materials, activated carbon with good CO₂ adsorption capacity was prepared by dry chemical modification [7]. Using rice husk, peanut shell, soybean straw and so on, biomass carbon was prepared with strong adsorption performance of methylene blue [8]. It has been rarely reported that the plant extract residue prepares porous carbon materials. Therefore, in this study, with the extract residue of tobacco stems as raw materials, after carbonizing, the biomass carbon porous materials were prepared by vacuum heat treatment with KOH as modifier. The effects of different mixing ratios of KOH and tobacco stalk residue after carbonizing on the surface structure and properties of activated carbon porous materials were studied. The adsorption effect of the modified materials on the harmful components of the cigarette smoke was also studied.

2. MATERIALS AND METHODS

Tobacco stem residue (TSR) was dried by microwave. The dried TSR was pulverized and filtered with an 850 µm screen.

The TSR was then placed in a tube furnace (GSL-1600X, Ningbo Oppl Instrument Co., Ltd., China) and heated at a rate of 5~20°C/min until 350°C for 30 min under nitrogen atmosphere. The TSR was cleaned by deionized water until the pH of the washing fluid became neutral. Then the TSR was conducted vacuum heat treatment at 90°C for 4h. KOH and TSR were put in tube furnace according to the quality of 1:1, 2:1 and 4:1 respectively, which were heated for 15 min at 600°C under nitrogen atmosphere, filtered and washed with HCl solution (mass fraction, 10%). And then it was cleaned by deionized water until the pH of the washing fluid became neutral. Finally, the resulting MTSR was dried at 110°C to a constant mass, filtered with a 850 µm screen, placed in polyethylene bags and stored in a dryer.

The surface morphologies of the samples were examined by field emission scanning electron microscopy (QUANTA-TA200, FEI, USA). The pore properties of the samples were estimated by nitrogen adsorption-desorption isotherms at 77 K using the specific surface areas and pore-size analyzer (NOVA2200e, Quanta chrome, USA). The Multipoint Brunauer-Emmett-Teller (BET) equation was used to calculate specific surface area of the samples. The total pore volume was acquired from the adsorptive amount of nitrogen at P/P0 = 0.98. Organic functional groups were characterized by Fourier transform infrared analysis (Bruker TENSOR27, BRUKER, Germany).

To assess the filtration properties of these carbons when incorporated in cigarette filters, the cigarette filters were prepared as follows: 60 ± 1 mg of the carbon granules were weighed into the cavity of a cigarette filter of a 24.6-mm circumference cigarette, made up of a 56-mm long

cigarette rod containing a Virginia-style tobacco blend (tobacco rod density of 255 mg cm⁻³ at a

moisture content of 13%) and a 27-mm length three-part cavity filter (10 mm cellulose acetate at

the rod end, 4-mm cavity and 13 mm cellulose acetate at the mouth end). Triacetin is used as a

plasticizer on cellulose acetate filter sections and loadings of 10% and 6% by weight for the mouth end and rod end segments, respectively, were used. Cigarette filters were all unventilated (i. e. no air vent holes are made to allow influx of air during puffing). A standard 50 CU permeability cigarette paper was used throughout [where 1 CU is the flow of air (cm³/minute) passing through 1 cm² surface of the test piece at a measuring pressure of 1.00 KPa]. As a control, cigarettes of the same dimensions and composition were also prepared with an empty 4-mm filter cavity section. To mimic manufacturing conditions, the cigarettes were conditioned at 22 °C and 60% relative humidity for 3 weeks following the inclusion of carbon in the cigarette filter and then smoked under ISO smoking conditions (one 35-ml volume puff of 2-second duration taken every minute) (International Organisation for Standardization 1991; Thomsen 1992). According to GB5606. 4-2005 [9], sensory evaluation was evaluated by professional assessment staffs.

Standard Test Method for determination of nicotine, tar and CO content in cigarette smoke: determination of total particulate matter and tar in GB/T19609-2004 cigarette by routine analysis with cigarette smoking machine [10]. Standard method for the determination of mainstream cigarette smoke: cigarette mainstream smoke in GB5606. 5-2005 [11]. Determination of phenol in mainstream cigarette smoke in 255-2008 YC/T cigarettes- high performance liquid chromatographic method [12].

3. RESULTS AND DISCUSSIONS

3.1 Experimental results and analysis of response surface

3.1.1 Experimental results of response surface

In view of the specific surface area of the porous material, the optimization scheme and the results of Box - Behnken test with three factors of processing temperature, ratio of raw materials to KOH and processing time are shown in Table 1, The design of a total of 17 test points, including 12 analysis points, 5 center points. The central point of repeated the purpose is to estimate pure experimental error of the whole experiment. Specific surface area of Y is the response value of the response surface analysis.

Table 1. Box- Behnken design test results of granulation of porous materials

Number	Encoding factors			Specific surface area Y/m ² /g
	Temperature X ₁ /°C(°C)	Ratio X ₂	Time X ₃ /min	
1	0(700)	0(1:3)	0(20)	1456.2
2	-1(600)	0(1:3)	-1(10)	1145.8
3	0(700)	0(1:3)	0(20)	1466.7
4	0(700)	1(1:4)	-1(10)	1256.4
5	0(700)	0(1:3)	0(20)	1423.9
6	1(800)	1(1:4)	0(20)	1140.7
7	0(700)	0(1:3)	0(20)	1439.2
8	-1(600)	-1(1:2)	0(20)	996.3
9	1(800)	0(1:3)	1(30)	1149.2
10	0(700)	1(1:4)	1(30)	1228.5
11	0(700)	-1(1:2)	1(30)	973.3
12	1(800)	0(1:3)	-1(10)	1183.8
13	-1(600)	1(1:4)	0(20)	1250.3
14	-1(600)	0(1:3)	1(30)	952.7
15	0(700)	-1(1:2)	-1(10)	1395.5
16	1(800)	-1(1:2)	0(20)	1238.6
17	0(700)	0(1:3)	0(20)	1423.6

3.1.2 Experimental results of response surface

The test data in table 1 was carried out of multiple regression fitting by MATLAB software. The temperature X₁, the ratio of X₂ and the time X₃ was the independent variables, the specific surface area (Y) was the response value, the fitting was obtained by the two multinomial regression model:

$$Y = 1451.32 + 45.90X_1 + 34.03X_2 - 84.73X_3 - 87.98X_1X_2 + 39.63X_1X_3 + 98.58X_2X_3 - 200.20X_1^2 - 94.65X_2^2 - 143.25X_3^2$$

The results of variance analysis of the regression model are shown in table 2. The response factor interaction on pelleting efficiency surface analysis and contour analysis results shown in Figure 1 to figure 4. From table 2 and figure 1 to figure 4

can be seen that the overall model has statistical significance, and the fitting effect comparison. The interaction between the

factors of the table area is significant intuitively from the figure 1 to figure 4.

Table 2. Variance analysis of regression coefficient

Model	Unstandardized coefficients		Standardized coefficients Beta	t	P	Sig.
	B	Std. error				
Constant	1451.320	19.465		74.562	.000	**
X ₁	45.900	15.388	.184	2.983	.020	*
X ₂	34.025	15.388	.137	2.211	.033	*
X ₃	-84.725	15.388	-.340	-5.506	.001	**
X ₁ X ₂	-87.975	21.762	-.250	-4.043	.005	**
X ₁ X ₃	39.625	21.762	.112	1.821	.061	
X ₂ X ₃	98.575	21.762	.280	4.530	.003	**
X ₁₂	-200.198	21.211	-.585	-9.438	.000	**
X ₂₂	-94.648	21.211	-.276	-4.462	.003	**
X ₃₂	-143.247	21.211	-.418	-6.753	.000	**

Note: *significant, **extremely significant.

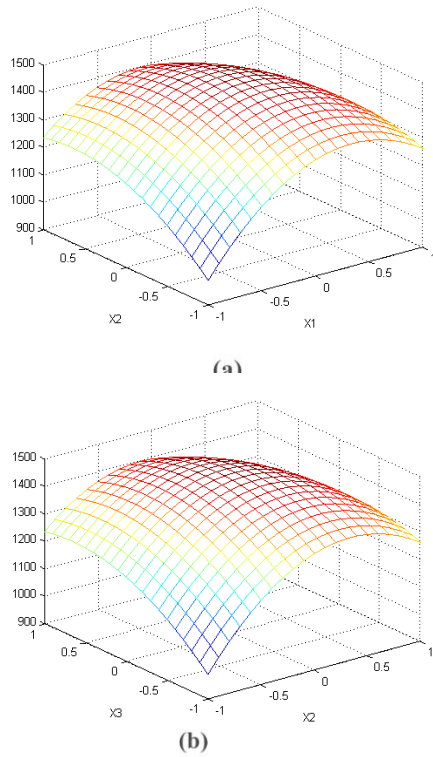


Figure 1. response surface analysis of (a) temperature and ratio (b) ratio and time to surface area

From table 2, we can see that the difference of X₁, X₂ is significant (P<0.05), the difference of X₃ is very significant (P<0.01), and the quadratic X₁₂, X₂₂ and X₃₂ arrived to a very significant level (P<0.01). The results showed that temperature, proportion and time has significant effect on the specific surface areas. The difference of the interaction X₁X₂ and X₂X₃ is very significant (P<0.01), which indicated that the interaction of temperature and proportion, proportion and time has a significant effect on the surface areas. The influence of the three factors on the the surface areas is: X₁>X₂>X₃(temperature > ratio > time). The excellent produced conditions for the adsorption materials are as

follows: the temperature is 707.40 °C, the ratio is 1:3 and the time is 17.20 min.

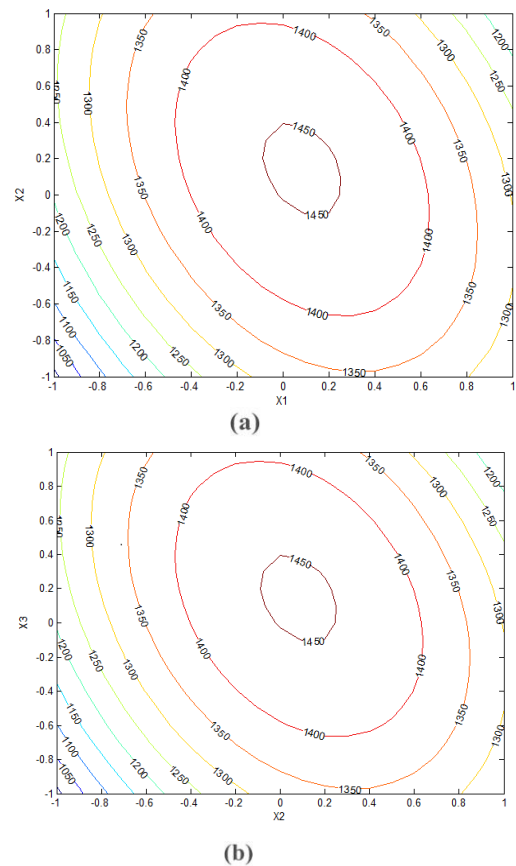


Figure 2. The contour of (a) temperature and ratio (b) ratio and time to surface area

2. 2 Microscopic morphology

The SEM images analysis results of EG and EGK are given in Figure 3. Figure 3(a) shows the surface morphology of EG. The results show that the surface is rough, and the shape of the strip shape is irregular. Figure 3(b) shows the surface morphology of EGK. It can be seen that the surface exhibits a large number of holes and pores after modifying treatment. The pore distribution is disordered and irregular,

and the holes connected to each other to form a network. The reason for the results is that chemical reactions occur between the materials and KOH during the thermal treatment. From Figure 1, the surface morphology of the material changes significantly and obtains a lot of cavities and pores by modifying treatment, which obviously increases the specific surface area. Greater specific surface areas are generally correlated with better adsorption performance. Therefore, the structure of the sample is better for adsorption.

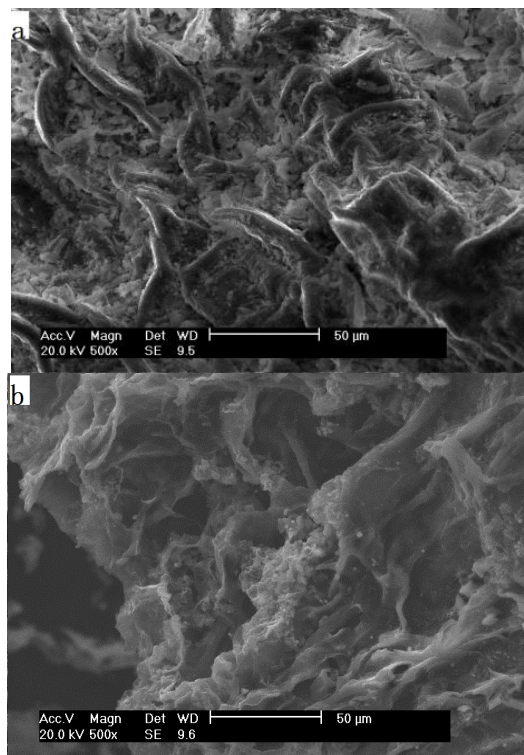


Figure 3. SEM images of EG(a) and EGK(b)

3.3 Microscopic structure

The Brunauer-Emmett-Teller test was carried out on the samples and the results are shown in Table 3. The results show that the specific surface areas and pores volumes (V_{total}) of EGK significantly increased to $1613.27 \text{ m}^2/\text{g}$ and $0.67 \text{ cm}^3/\text{g}$ respectively. This dramatic increase in surface areas and pore volumes are as a result of the chemical reactions occurring between KOH and EG. The reactions are given below.

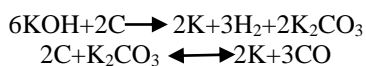


Table 3. Structural characteristic of the materials before and after modification

	EG	EGK
$S_{BET}(\text{m}^2/\text{g})$	17.32	1613.27
$V_{total}(\text{cm}^3/\text{g})$	0.01	0.67

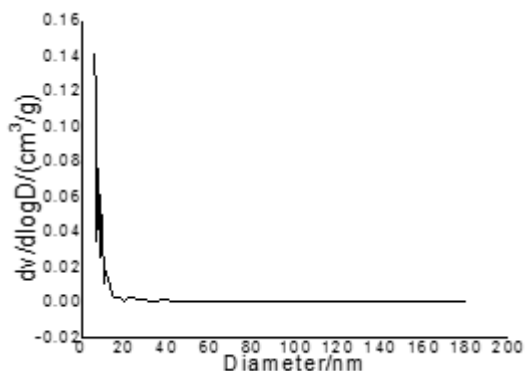


Figure 4. Pore size distribution of EGK

The adsorption properties of porous materials are greatly affected by the pore-size distribution. Thus, the pore-size distribution was investigated and the results are shown in Figure 4. It can be seen that the pore size is mainly concentrated in the range of $6 \sim 15 \text{ nm}$, which indicates that the pore structure is mainly based on the larger mesoporous structure and has certain smaller microporous structure [11-15]. In addition, some studies have shown that the pore size of aporous material determines the specific surface areas and pore volumes of the material, which affects its adsorption capacity [16]. The smaller pore size is better for adsorption, but very small pore sizes can be blocked by the adsorbate. Therefore, the pore size of EGK is suitable for adsorbate channels, with capillary condensation under certain pressures, which is better for the adsorption of large molecules.

3.4 Surface characteristics

Some studies have shown that functional groups and dangling bonds have a greater impact on the adsorption [17]. The FTIR spectrograms of EG and EGK are shown in Figure 5. Special functional groups corresponding to the absorption position were analyzed according to the literatures [18, 19]. In the FTIR analysis, the strong peak near 3418.13 cm^{-1} is attributed to the hybrid stretching vibration of O-H and N-H, and the peak near 2923.08 cm^{-1} is probably the peak of CH^2 and CH^3 . The strong peak near 1637.03 cm^{-1} is the N-H stretching vibration of the primary amine, the strong peak near 1032.58 cm^{-1} is the absorption band of the C-O-C symmetric and asymmetric stretching vibrations and the O-H unbalanced surface rocking vibration of the carboxyl group molecular aggregates, and the peak near 606.05 cm^{-1} is the absorption band of SO_4^{2-} . According to the above analysis, the material has many functional groups, such as hydroxyl, amine, and carboxyl groups and non-carbon elements. These kinds of functional groups could result in improving polar, hydrophilic, catalytic performance and changing the surface charge, which can enhance the interaction between the adsorbent and adsorbate. Thus, the porous material will have a better adsorption capacity [20].

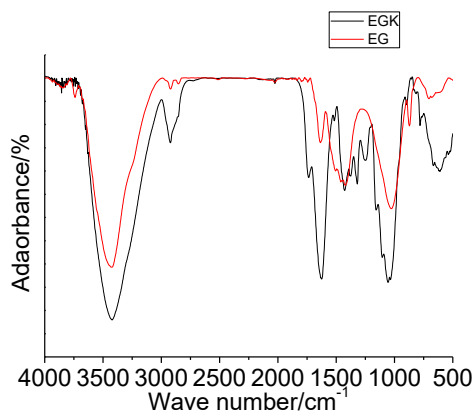


Figure 5. IR spectra of porous materials before and after modification

Comparison of the FTIR spectrograms of EG and EGK are roughly similar regardless of treatment condition, but the intensity of each stretching vibration peak significantly changed after modification, which indicates that modification can increase the functional groups of -OH and -CH. It shows that the material has a certain pro organic.

3.5 Effect of EGK dosage on the harmful components of smoke

Table 4 is the results of main components of smoke. Compared with control cigarettes, the smoke of cigarettes added 20mg, 30mg and 40mg of EGK were obviously decreased. When EGK was added 30mg, tar, CO and phenol decreased 20.5%, 19.2% and 49.66% respectively. At this time the adsorption of harmful components reached the highest. Nicotine in smoke decreased 7.34%. Continue to increase the amount, the adsorption remained unchanged. According to the analysis, the abundant pores and net structures of EGK could result in increasing a large number of specific surface areas and pore volumes which increases the probability of retention of aerosols.

And the EGK prolong the residence time in the filter through interfering the movement of aerosol particles. Thus, the EGK has higher filtration efficiency [21-23]. EGK has a large number of hydroxyl functional groups, which can be used in the hydrogen bonding interaction with hydroxyl groups in phenol. At the same time, -CH and other organic functional groups could result in changing the surface polarity, increasing the active site of the nonpolar phenol molecules. Therefore, the phenol of smoke can be effectively reduced. While, the existence form of nicotine is the same as the particle phase, but its good volatile make it easy to be washed by fresh flue gas. Thus, the filter effect of EGK on nicotine is not very obvious.

Table 4. General indexes of cigarette

sample	Tar /mg/ branch	Nicotine /mg/ branch	CO/mg/ branch	Phenol / μ g / branch
Control sample	11.65	1.09	12.75	4.35
EGK—20	10.53	1.05	10.16	2.92
EGK—30	9.26	1.01	9.95	2.17
EGK—40	9.28	1.01	9.94	2.18

Note: The values of the content are the average values from three duplicate tests.

3.6 Adsorption time on the adsorption of phenol

In order to analyze the influence of different adsorption time of EGK on the adsorption of phenol, added EGK to the filter according to the amount of 30mg/ branch. The relation curve is shown in figure 6. With increasing time, the adsorption amount of EGK on phenol increases, which indicates that the flow rate of aerosol in the unit time is quantitative. The adsorption capacity of EGK on phenol directly affected by the velocity through the filters.

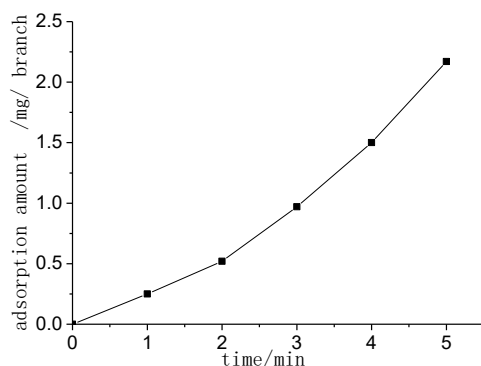
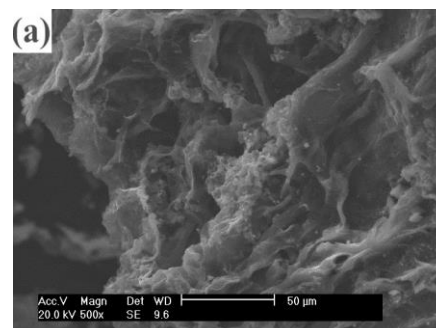


Figure 6. adsorption capacity of phenol with different contact times of EGK

3.7 Morphology of the materials before and after adsorption

Figure 7 is the surface morphology of the material before and after adsorption. The holes of the surface were almost fully occupied after the adsorption. Because the phenol is exist in the form of aerosol, and the size of aerosol particles is not uniform, which results in smaller particles getting into the void, the larger particles adsorbing in the external. Finally, the holes will be filled up.



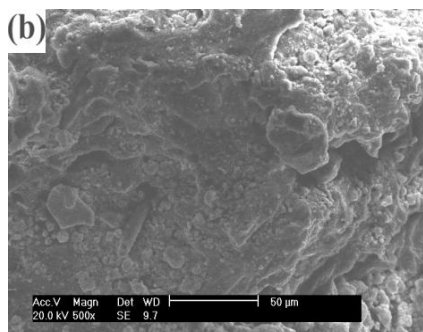


Figure 7. SEM diagram of the material before and after adsorption

4. CONCLUSIONS

In order to obtain biomass based porous materials of higher porosity and specific surface areas, extracted the tobacco stem, then the residue was modified by KOH. The effect of modification treatment on the morphology, structure and surface properties of the materials was analyzed. According to the experimental results, we can draw the following conclusions:

(1) By response surface method, temperature, proportion and time of the porous materials with specific surface area of the porous materials were obtained by two multinomial regression equation model. The excellent produced conditions for the porous materials are as follows: the temperature is 707.40 °C, the ratio is 1:3 and the time is 17.20 min. The analysis of variance shows that the equation can well analyze and predict the specific surface area of porous materials.

(2) The surface structure of EG was obviously affected by the KOH modification treatment. The EGK through modifying has a large number of holes and pores, and the holes connected to each other formed a network. Because of the chemical reaction between KOH and EG, the specific surface area and pore volumes of EGK increased significantly, which reached to 1513.27 m²/g and 0.67 cm³/g, respectively. Thus, the materials have better adsorption effect.

(3) Due to the rich holes and reticular structure of EGK, Retention probability of EGK on aerosols was significantly increased. Thus, tar and CO in the aerosols was better adsorbed. EGK has a large number of –OH and –CH functional groups, which can be used in the hydrogen bonding interaction with hydroxyl groups of phenol or changed the surface polarity, increasing the active sites of the nonpolar phenol molecules. Therefore, the phenol of smoke can be effectively reduced.

ACKNOWLEDGMENTS

This work was supported financially by China Tobacco Yunnan Industrial Co., Ltd. (project number: 2013CP02-2014158)

REFERENCES

- [1] Z. G. Chen, L. S. Zhang, Y. W. Tang, et al., "Adsorption of nicotine and tar from the mainstream smoke of cigarettes by oxidized carbon nanotubes," *J. Applied Surface Science*, vol. 252, no. 8, pp. 2933–2937, 2006. DOI: [10.1016/j.apsusc.2005.04.044](https://doi.org/10.1016/j.apsusc.2005.04.044).
- [2] C. Nie, L. E. Zhao, B. Peng, et al., "Studies on post-synthesized amine-functionalized materials for reducing volatile carbonyl compounds in cigarette smoke," *J. Acta Tabacaria Sinica*, vol. 16, no. B 12, pp. 50–54, 2010.
- [3] Q. B. Wen, C. T. Li, Z. H. Cai, et al., "Study on activated carbon derived from sewage sludge for adsorption of gaseous formaldehyde," *J. Bioresource Technology*, vol. 102, no. 2, pp. 942–947, 2011. DOI: [10.1016/j.biortech.2010.09.042](https://doi.org/10.1016/j.biortech.2010.09.042).
- [4] D. Chen, Z. Qu, Y. Sun, et al., "Adsorption-desorption behavior of gaseous formaldehyde on different porous Al₂O₃ materials," *J. Colloids & Surfaces A Physicochemical & Engineering Aspects*, vol. 441, no. 3, pp. 433–440, 2014. DOI: [10.1016/j.colsurfa.2013.10.006](https://doi.org/10.1016/j.colsurfa.2013.10.006).
- [5] W. Chen, X. Sun, Q. Cai, et al., "Facile synthesis of thick ordered mesoporous TiO₂ film for dye-sensitized solar cell use," *J. Electrochemistry Communications*, vol. 9, no. 3, pp. 382–385, 2007. DOI: [10.3969/j.issn.0438-1157.2013.09.036](https://doi.org/10.3969/j.issn.0438-1157.2013.09.036).
- [6] E. A. Dawson, M. B. Parkes Gareth, P. Branton. "Synthesis of vegetable-based activated carbons with mixed micro- and mesoporosity for use in cigarette filters," *J. Adsorption Science & Technology*, vol. 30, no. 10, pp. 859–866, 2012. DOI: [10.1260/0263-6174.30.10.859](https://doi.org/10.1260/0263-6174.30.10.859).
- [7] A. Alabadi, S. Razzaque, Y. Yang, et al., "Highly porous activated carbon materials from carbonized biomass with high CO₂ capturing capacity," *J. Chemical Engineering Journal*, vol. 281, pp. 606–612, 2015. DOI: [10.1016/j.cej.2015.06.032](https://doi.org/10.1016/j.cej.2015.06.032).
- [8] Xu R. B., Zhao A. Z., Xiao S. C., et al., "The adsorption of methylene blue in water by biomass char prepared from crop residues," *J. Environmental Science*, vol. 33, no. 1, pp. 142–146, 2012.
- [9] State Tobacco Monopoly Bureau. GB 5606. 4-2005. Cigarette sensory technology requirements.
- [10] GB/T19609-2004 Determination of total particulate matter and tar in cigarette by routine analysis.
- [11] National Tobacco Monopoly Bureau GB 5606. 5-2005. Cigarette mainstream smoke.
- [12] YC/T 255-2008 Determination of phenolic compounds in mainstream cigarette smoke by high performance liquid chromatography.
- [13] Z. H. Zhang, S. M. Xie, M. Zhang, et al., "Novel inorganic mesoporous material with chiral nematic structure derived from nanocrystalline cellulose for high-resolution gas chromatographic separations," *J. Analytical Chemistry*, vol. 86, no. 19, pp. 9595–602, 2014. DOI: [10.1021/ac502073g](https://doi.org/10.1021/ac502073g).
- [14] S. H. Joo, S. J. Choi, I. Oh, et al., "Ordered nanoporous arrays of carbon supporting high dispersions of Platinum nanoparticles" *J. Nature*, vol. 412, no. 6843, pp. 169–172, 2001. DOI: [10.1038/35084046](https://doi.org/10.1038/35084046).

- [15] L. Y. Yuan, Y. L. Liu, W. Q. Shi, et al., "A novel mesoporous material for uranium extraction, dihydroimidazole functionalized SBA-15," *J. Journal of Materials Chemistry*, vol. 22, no. 33, pp. 17019-17026, 2012. DOI: [10.1039/C2JM31766D](https://doi.org/10.1039/C2JM31766D).
- [16] W. Zhang, G. Ye and J. Chen. "Novel mesoporous silicas bearing phosphine oxide ligands with different alkyl chains for the binding of uranium in strong HNO₃ media," *J. Journal of Materials Chemistry A*, vol. 1, no. 41, pp. 12706-12709, 2013. DOI: [10.1039/C3TA13028B](https://doi.org/10.1039/C3TA13028B).
- [17] S. P. Sturgis. "A spectral-analysis tutorial with examples in FORTRAN," *J. Behavior Research Methods & Instrumentation*, vol. 15, no. 3, pp. 377-386, 1983. DOI: [10.3758/BF03203663](https://doi.org/10.3758/BF03203663).
- [18] R. Gong, Y. Sun, J. Chen, et al., "Effect of chemical modification on dye adsorption capacity of peanut hull," *J. Dyes and Pigments*, vol. 67, no. 3, pp. 175-181, 2005. DOI: [10.1016/j.dyepig.2004.12.003](https://doi.org/10.1016/j.dyepig.2004.12.003).
- [19] R. P. Han, W. H. Zou, J. H. Zhang, et al., "Characterization of chaff and biosorption of copper and lead ions from aqueous solution," *J. Acta Scientiae Circumstantiae*, vol., 26, no. 1, pp. 32-39, 2006. DOI: [10.331/j.issn:0253-2468.2006.01.006](https://doi.org/10.331/j.issn:0253-2468.2006.01.006).
- [20] Y. Xia, R. Mokaya, G. S. Walker, et al., "Superior CO₂ adsorption capacity on Ndoped, high-surface-area, microporous carbons templated from zeolite," *J. Adv. Energy Mater*, vol. 1, no. 4, pp. 678-683, 2011. DOI: [10.1002/aenm.201100061](https://doi.org/10.1002/aenm.201100061).
- [21] J. H. Zhang, S. M. Xie, M. Zhang, et al., "Novel inorganic mesoporous material with chiral nematic structure derived from nanocrystalline cellulose for high-resolution gas chromatographic separations," *J. Analytical Chemistry*, vol. 86, no. 19, pp. 9595-9602, 2014. DOI: [10.1021/ac502073g](https://doi.org/10.1021/ac502073g).
- [22] Y. Xia, R. Mokaya, G. S. Walker, et al., "Superior CO₂ adsorption capacity on n-doped, high-surface-area, microporous carbons templated from zeolite," *J. Advanced Energy Materials*, vol. 1, no. 4, pp. 678-683, 2011. DOI: [10.1002/aenm.201100061](https://doi.org/10.1002/aenm.201100061).
- [23] M. A. Nahil and P. T. Williams. "Pore characteristics of activated carbons from the phosphoric acid chemical activation of cotton stalks," *J. Biomass & Bioenergy*, vol. 37, no. 1, pp. 142-149, 2012. DOI: [10.1016/j.biombioe.2011.12.019](https://doi.org/10.1016/j.biombioe.2011.12.019).